

## Peierls-Nabarro model of dislocations in silicon with generalized stacking-fault restoring forces

B. Joós\* and Q. Ren†

*Ottawa Carleton Institute of Physics, University of Ottawa Campus, Ottawa, Ontario, Canada K1N 6N5*

M. S. Duesbery‡

*Fairfax Materials Research Inc., 5613 Marble Arch Way, Alexandria, Virginia 22310-4011*

(Received 23 March 1994)

Using generalized stacking-fault (gsf) energies obtained from first-principles density-functional calculations, a zero-temperature model for dislocations in silicon is constructed within the framework of a Peierls-Nabarro (PN) model. Core widths, core energies, PN pinning energies, and stresses are calculated for various possible perfect and imperfect dislocations. Both shuffle and glide sets are considered. 90° partials are shown to have a lower Peierls stress than the 30° partials in accord with experiment.

### I. INTRODUCTION

There are several reasons why the study of dislocations in silicon is important. In Si, an elemental covalent semiconductor crystallizing in the diamond structure, the dislocations have a high-energy and high-frictional resistance. This makes it rather easy to grow crystals with a low dislocation density. Since plastic glide occurs by dislocation motion, Si and, as a matter of fact, the other elements in the same column of the Periodic Table having the diamond structure, are ideal systems for the study of plastic deformation. On the other hand, over the last few years a new generation of optoelectronic devices has been developed from heterostructures made from lattice mismatched Si-Ge alloys.<sup>1</sup> The performance of these devices can be severely impaired by the presence of dislocations. Understanding the properties of these defects is therefore crucial in the design of the new devices.

Quite a few reviews discuss dislocations in Si (see Refs. 2–7), which have been studied for many years. Although the experimental studies are extensive, a comprehensive picture of dislocation generation and mobility is not yet available. The overall geometry and topology of the core structures are understood, but little has been done quantitatively on the microscopic properties. In particular, no estimate so far has been published for the Peierls stress of the dislocations. Modeling dislocations is intrinsically difficult because of the large unit cells required. First-principles pseudopotential calculations are prohibitive. Several classical empirical potentials have recently been proposed for Si and have been used to model many properties. These potentials have, however, so far failed to produce a realistic picture of the dislocation structures.<sup>8,9</sup> The recent first-principles calculations of the generalized stacking fault (gsf) energies<sup>10,11</sup> have provided reliable values for the restoring forces occurring close to the core of a dislocation. We have used these results to compute the low-temperature dislocation profiles, core energies, and Peierls stresses for the full and partial dislocations of Si within the framework of the Peierls-Nabarro (PN) model. Vitek and co-workers<sup>12–14</sup> have compared the results of this model with those of atomistic calculations

and have shown that for planar dislocations it gives reasonable results.

The outline of the paper is as follows. In the next section we review and summarize the known properties of dislocations in Si. In Sec. III, the dislocation model used, the Peierls-Nabarro (PN) model,<sup>15–17</sup> is presented and discussed. Section IV presents our solutions of dislocation profiles, and Sec. V the results on misfit energies, PN energies and stresses. A discussion and conclusion ends the paper.

### II. DISLOCATIONS IN SILICON

The diamond cubic structure into which Si crystallizes is formed of two interpenetrant face-centered-cubic (fcc) lattices. The dislocations are, therefore, expected to be similar in these two crystal structures. In the fcc lattice the main slip plane is the {111} plane and the major slip direction is  $\langle 110 \rangle$ . The smallest Burgers vector is  $\frac{1}{2}\langle 110 \rangle$ . At high temperatures slip has also been observed in the {110} and {100} planes along the same  $\langle 110 \rangle$  directions. There is a low-energy stacking fault in the {111} plane for displacement of  $\frac{1}{6}\langle 2\bar{1}\bar{1} \rangle$ . This permits the dissociation of the perfect dislocations into two imperfect dislocations with partial Burgers vectors. For instance,

$$\frac{1}{2}\langle \bar{1}0\bar{1} \rangle \rightarrow \frac{1}{6}\langle \bar{2}11 \rangle + \frac{1}{6}\langle \bar{1}\bar{1}2 \rangle . \quad (1)$$

Such decomposition reduces dilation and compression on both sides of the slip plane. The imperfect dislocations obtained are glissile on the (111) plane and are known as Shockley partials. These partials are separated by a stacking fault, whose size is determined by the balance of the  $1/r$  repulsion between the partials with the attractive force resulting from the stacking fault.

The above characteristics are also found in the diamond lattice. The stacking-fault energy is, however, expected to be even lower than in the fcc lattice. In the diamond-lattice atomic layers come in pairs. So instead of having distortions in the second-nearest-neighbor planes the distortions in the bonds occur in the fourth-

nearest-neighbor planes. And since, in a covalently bond structure such as the diamond lattice, atoms interact mainly with their nearest neighbors, these interactions will be weak. For Si one typically quoted value for the intrinsic stacking fault energy is  $69 \text{ mJ/m}^2$  or  $55 \text{ meV/unit cell area}$ .<sup>5,17</sup>

In both the fcc and diamond cubic lattices there are two perfect dislocations with Burgers vectors and dislocation lines along  $\langle 110 \rangle$  directions, a pure screw and a  $60^\circ$  dislocation, the latter term arising from the  $60^\circ$  angle between the direction of the dislocation line and the Burgers vector. The difference is that in the diamond cubic lattice there are in principle two distinct  $\{111\}$  glide planes (see Fig. 1), one called the glide plane, situated in between two close-packed planes of different index, and the other the shuffle plane, separating two planes of the same index cutting through bonds oriented perpendicularly to the  $\{111\}$  plane. These two planes lead to two sets of dislocations. The glide set, with properties very similar to those observed in the fcc lattice, can dissociate into two partials separated by a low-energy stacking fault; for the screw two  $30^\circ$  partials and for the  $60^\circ$ , a  $30^\circ$ , and a  $90^\circ$  partial. They derive their name from the fact that they are believed to undergo glide in the sense of continuum dislocations. This is not the case for the shuffle set, which breaks up two planes of the same index and has no low-energy stacking fault. The dissociation into partials in this case is more complex, and their motion has been argued to be akin to a shuffling motion involving movement of interstitials.<sup>17</sup>

The core structures have been discussed in detail in several review articles (in particular in Ref. [4]), but the accepted models are not fully consistent with images in high-resolution electron microscopy. Measurements of dislocation mobilities and of electrical activities do not clarify the situation but bring added confusion. We will not discuss these points here but refer to two recent reviews.<sup>5,6</sup> We will only mention some points relevant to our calculation. Because of covalent bonding, which re-

quires high energy to break or to distort the bond angle, dislocations are expected to be narrow in the diamond structure. Dangling bonds in the core are reconstructed as on surfaces. The width of the stacking fault separating the two partials in a dissociated dislocation is about  $40 \text{ \AA}$  for the screw dislocation and  $65 \text{ \AA}$  for the  $60^\circ$  dislocation.<sup>18</sup> So we would expect the partials to be nearly decoupled. Experiments by a group in Köln<sup>19,20</sup> and later by another in Poitiers<sup>21,22</sup> put them rather in an intermediate regime between "bound" and "torn away" (using terminology of Ref. 17). Under applied stress the width of a  $60^\circ$  glide dislocation is observed to be increased if the  $90^\circ$  partial leads and to be narrowed if the  $30^\circ$  partial does. The screw formed of two  $30^\circ$  partials seems to remain fairly narrow.<sup>21,22</sup> The dissociation widths depend on the orientation of the stress. One clear conclusion can be drawn, the  $90^\circ$  partial is more mobile than the  $30^\circ$  partial.

In the study that follows we will look at the full dislocations in both the glide and shuffle planes and the two partials in the glide plane. These are the dislocations whose glide are expected to be controlled by the Peierls-Nabarro mechanism. The shuffle partials involve motions difficult to incorporate in a Peierls-Nabarro model.

### III. THE PEIERLS-NABARRO MODEL

To facilitate the presentation we will adopt the following conventions in all that follows (see Fig. 2). In a Cartesian set of coordinates  $xyz$ , the  $xOz$  plane is the glide plane  $\{111\}$ . The  $z$  axis is the direction of the dislocation line (a  $\langle 110 \rangle$  line), the  $x$  axis the direction perpendicular to it within the glide plane (the glide direction or  $\langle 112 \rangle$ ) and finally the  $y$  axis is the normal to the glide plane. The Burgers vector lies in the glide plane making an angle  $\theta$  with the  $z$  axis. The dominant direction of displacement of the atoms around the dislocation line is along the Burgers vector. For a pure edge dislocation the Burgers vector would lie along the  $x$  axis (or  $\theta=90^\circ$ ), while for a pure screw dislocation along the  $z$  axis (or  $\theta=0^\circ$ ). A dislocation with any other angle would be mixed, partly edge and partly screw. Its Burgers vector can be decomposed into two components, one along the  $x$  axis, the

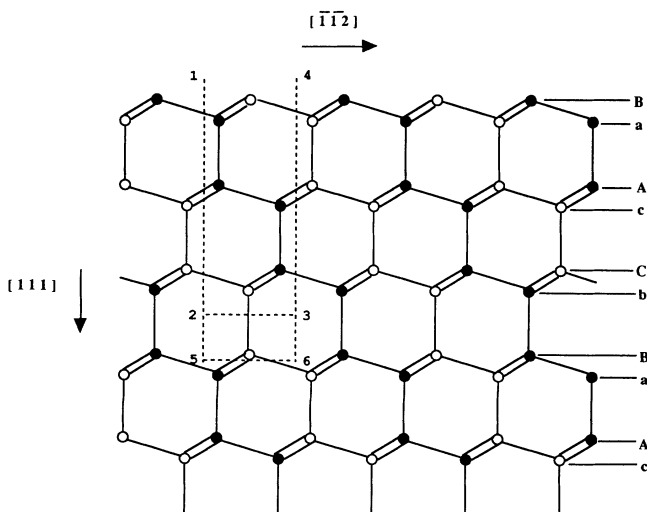


FIG. 1. A diamond-cubic lattice projected normal to a  $[1\bar{1}0]$  plane.

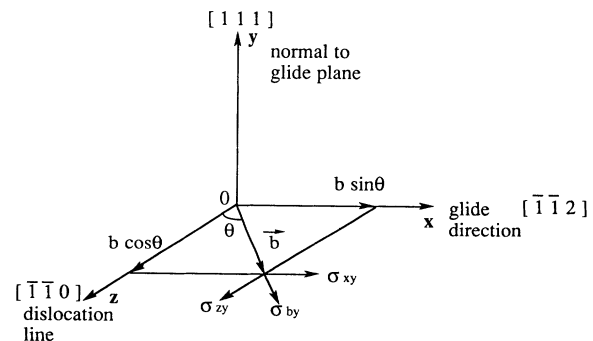


FIG. 2. A Cartesian set of coordinates showing the directions relevant for dislocations in silicon. With the above choice of axes,  $\theta=60^\circ$  gives  $\mathbf{b}$  along  $[\bar{1}01]$  and  $\theta=30^\circ$  along  $[\bar{2}11]$ .

edge component  $b \sin\theta$ , and the other along the  $z$  axis, the screw component  $b \cos\theta$ .

A continuum theory has been developed, which can be fully solved (see, for instance, Ref. 17). For future purposes, let us just note that for an isotropic crystal an edge dislocation produces in its glide plane, whose normal is along the  $y$  axis, a stress field  $\sigma_{xy}$  along its Burgers vector; here the  $x$  direction (and hence the two suffixes  $xy$ ):

$$\sigma_{xy} = \frac{\mu b}{2\pi(1-\nu)} \frac{1}{x}, \quad (2)$$

where  $\mu$  is the shear modulus and  $\nu = \frac{1}{2}\lambda/(\lambda + \mu)$ , the Poisson ratio expressed in terms of the conventional Lamé constants  $\lambda$  and  $\mu$ .

Similarly, for a screw dislocation, whose Burgers vector is along the  $z$  direction, the stress along  $z$  in the glide plane is

$$\sigma_{zy} = \frac{\mu b}{2\pi} \frac{1}{x}. \quad (3)$$

For a mixed dislocation with a Burgers vector  $\mathbf{b}$  making an angle  $\theta$  with the  $z$  axis, the component of its stress field along the Burgers vector is given by

$$\sigma_{by} = \sigma_{xy} \sin\theta + \sigma_{zy} \cos\theta = \frac{\mu b}{2\pi} \left[ \frac{\sin^2\theta}{(1-\nu)} + \cos^2\theta \right] \frac{1}{x}. \quad (4)$$

In the continuum model a dislocation can be displaced without any application of force because the effects of the lattice periodicity are not included. In the Peierls-Nabarro (PN) model they are included, for their essential part, in the following way. When a dislocation is present there is a natural interface defined by the glide plane in which the dislocation line lies. The PN model balances at this interface the stress fields predicted by continuum theory with the crystal restoring forces across the interface. The implicit assumption is that the core, the region of inelastic displacements, is spread along the glide plane. This is known to be a good approximation for fcc-type lattices.<sup>7</sup> Specifically, at each point at a distance  $x$  from the dislocation line, the stress generated by the displacement  $f$  of the upper half of the crystal ( $y > 0$ ) with respect to the lower half ( $y < 0$ ) is viewed as being due to a continuous distribution of infinitesimal dislocations at every point  $x'$  of Burgers vectors  $\rho(x')dx' = [df/dx]_x dx'$ . The component of this resultant stress  $\sigma_{by}(x)$  along  $\mathbf{b}$  is balanced by the corresponding component of the periodic restoring force stress  $F_b(f)$  acting between atoms on either side of the interface. This equilibrium condition leads to the integrodifferential equation known as the PN equation

$$\frac{K}{2\pi} \int_{-\infty}^{+\infty} \frac{1}{x-x'} \frac{df(x')}{dx'} dx' = F_b(f(x)), \quad (5)$$

with the normalization condition

$$\int_{-\infty}^{+\infty} \rho(x') dx' = \int_{-\infty}^{+\infty} \frac{df(x')}{dx'} dx' = b. \quad (6)$$

$K$  depends on the type of dislocation and the crystalline direction of the Burgers vector. For an isotropic crystal,  $K$  follows from Eq. (4):

$$K = \mu \left[ \frac{\sin^2\theta}{(1-\nu)} + \cos^2\theta \right]. \quad (7)$$

In the original PN model the restoring stress was taken to be sinusoidal with an amplitude determined by imposing the proper elastic slope. The problem has for this case an analytical solution worth mentioning because it is a reference and a starting point for the general case. The forms used in the original model for an edge dislocation and the general sinusoidal restoring stress are given below

$$\sigma_{xy}(x,0) = \frac{\mu b}{2\pi d} \sin \frac{2\pi f(x)}{b} = \tau_{\max} \sin \frac{2\pi f(x)}{b}, \quad (8)$$

where  $d$  is the interplanar spacing in the direction perpendicular to the interface, and  $\tau_{\max}$  is the maximum stress that can be generated at the interface. This gives the following PN equation:

$$\int_{-\infty}^{+\infty} \frac{1}{x-t} \frac{df(t)}{dt} dt = \frac{2\pi\tau_{\max}}{K} \sin \frac{2\pi f(x)}{b}. \quad (9)$$

Its solution is

$$f(x) = \frac{b}{\pi} \tan^{-1} \frac{x}{\xi} + \frac{b}{2} \quad (10)$$

or

$$\rho(x) = \frac{df(x)}{dx} = \frac{b\xi}{\pi(\xi^2 + x^2)}, \quad (11)$$

where  $\xi = Kb/(4\pi\tau_{\max}) = d/[2(1-\nu)]$  can be viewed as the half width of the dislocation, the region wherein the disregistry is greater than one-half its maximum value at  $x=0$ . This is similar to the solution for the Frenkel and Kontorowa<sup>23</sup> or Frank and van der Merwe<sup>24</sup> model of dislocations (see also Ref. 25). It gives a solitonlike profile with  $f(-\infty)=0$ ,  $f(0)=b/2$ , and  $f(\infty)=b$  (similar shapes are found in our solutions, see Fig. 5). With the above choice of solution, the lower half plane has an additional plane of atoms. With a negative sign on the  $\tan^{-1}$  term, the upper half plane is compressed.

It is to be noted that for every dislocation with sinusoidal restoring forces a solution identical to the one above will be obtained. What changes is only the direction of the displacement field, which is along the Burgers vector and, hence, the elastic constants, which govern the response of the lattice and the interface.

In an actual crystal the restoring forces may be quite different from sinusoidal. Foreman, Jaswon, and Wood<sup>26</sup> first considered the effect on dislocation properties of modifying the functional form of the restoring force. The major breakthrough was to derive the restoring force from the gsf energies as had been suggested by Christian and Vitek<sup>27</sup> and applied to bcc crystals by Lejček<sup>28</sup> and Kroupa and Lejček.<sup>29</sup> The gsf of interest to us is obtained by cutting the crystal along the  $\{111\}$  plane displacing one half with respect to the other by a vector  $\mathbf{f}$  and then rejoining them. The energies of the gsf generate

what is known as a  $\gamma$  surface  $\gamma(f)$  (energy per unit area). The restoring stress is simply

$$F(f) = -\frac{\partial\gamma}{\partial f}. \quad (12)$$

The gsf energies we are using have been obtained from a local-density approximation (LDA) to the density-functional theory (DFT), a first-principles calculation (for details see Refs. 10 and 11). Such calculations are computationally demanding. For this reason fully relaxed atomic configurations were considered for only two points, the lowest-energy barriers in the glide and shuffle planes, known as the unstable stacking-fault energies ( $\gamma_{us}$ ). In the glide plane this occurs at a displacement of  $\frac{1}{12}\langle 1\bar{2}1 \rangle$  in units of the repeat distance along this crystallographic direction. The metastable stacking fault or intrinsic stacking fault is at  $\frac{1}{6}\langle 1\bar{2}1 \rangle$ . For the shuffle plane the preferred slip paths are along  $\langle 110 \rangle$  directions and the unstable stacking fault occurs for a displacement of  $\frac{1}{4}\langle 110 \rangle$ . The relevant energies and forces are given in Table I. To construct the variation of the gsf over the two directions of interest, we have scaled the unrelaxed gsf energies by the decrease of the unstable stacking-fault energy for each surface. It is an approximation whose consequence would be hard to assess quantitatively. But we expect the relaxation to be the largest at the unstable stacking fault. Consequently our scaling procedure would tend to underestimate  $\gamma$  for small displacements. The important thing for our purposes is that the conclusions of the paper are unchanged whether unrelaxed or “relaxed”  $\gamma$  surfaces are used in the calculations, only the absolute values of the quantities are different as we have checked. Figure 3 gives our scaled gsf energies for the shuffle and glide planes along the directions of interest, while Fig. 4 shows the corresponding restoring stresses. The energy variations are seen to be mainly sinusoidal with comparable magnitudes for the segments relevant to the shuffle dislocations and glide partials [Fig. 3(b)], while the gsf energy variation relevant to the glide dislocations is an order of magnitude larger. The corresponding restoring stresses show slight departures from sinusoidal behavior, and their magnitudes are in direct correlation with the corresponding  $\gamma$  surface energy variations (see Fig. 4).

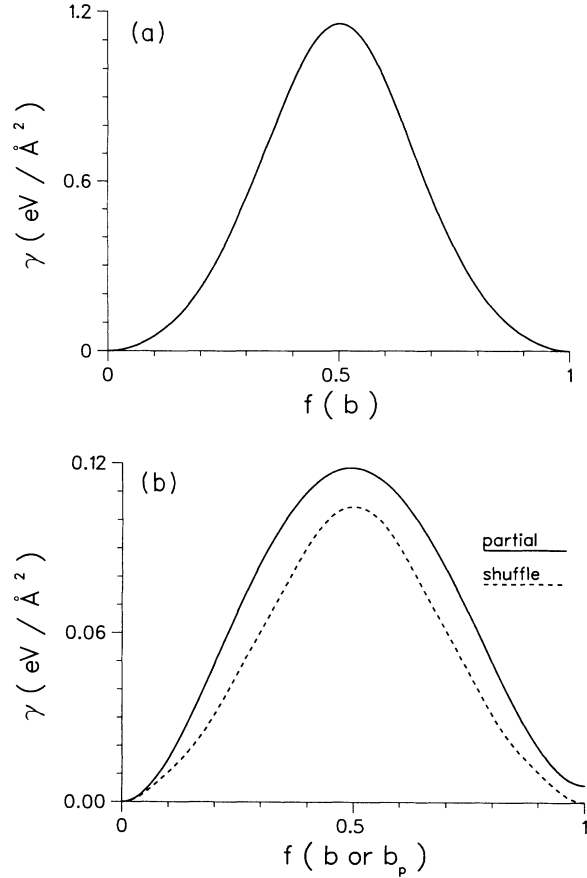


FIG. 3.  $\gamma$  surface sections (a) along a  $\{110\}$  direction in the glide plane and (b) dashed line along the same direction in the shuffle plane. Both cover a total displacement of a full Burgers vector  $b = 3.84 \text{ \AA}$ . The full line in (b) along a  $\{112\}$  direction of the glide plane is shown; at  $b_p = 2.22 \text{ \AA}$ , the Burgers vector for a glide partial, the stacking-fault energy is the energy of the intrinsic stacking fault  $0.006 \text{ eV/\AA}^2$ .

#### IV. DISLOCATION PROFILES

The solution to the PN equation, Eq. (5), requires knowledge of the  $K$  parameters and the restoring forces. The  $K$  parameters measure the elastic response of the lattice to displacements along the Burgers vector direction.

TABLE I. Key parameters characterizing dislocation properties.  $K$  measures the stiffness of the Si lattice for a given direction of distortion [see Eq. (7)].  $\gamma_{\max}$  is the maximum of the  $\gamma$  surface in the relevant interface along the direction of the Burgers vector  $\langle 110 \rangle$  for full dislocations and  $\langle 112 \rangle$  for partials.  $\tau_{\max}$  is the corresponding maximum restoring stress and  $2\xi$  is the calculated dislocation width but obtained using the criterion given in the text ( $1 \text{ eV/\AA}^3 = 1.6 \times 10^{12} \text{ dyn/cm}^3$ ).

Dislocation		$K$ ( $\text{eV/\AA}^3$ )	$\gamma_{\max}$ ( $\text{eV/\AA}^2$ )	$\tau_{\max}$ ( $\text{eV/\AA}^3$ )	$b$ ( $\text{\AA}$ )	$2\xi$ ( $\text{\AA}$ )
Glide	$60^\circ$	0.501	1.156	1.11	3.84	0.37
	Screw	0.400	1.156	1.11	3.84	0.30
Shuffle	$60^\circ$	0.501	0.105	0.08	3.84	3.95
	Screw	0.400	0.105	0.08	3.84	3.14
Glide	$30^\circ$	0.433	0.118	0.15	2.22	0.92
Partials	$90^\circ$	0.536	0.118	0.15	2.22	1.16

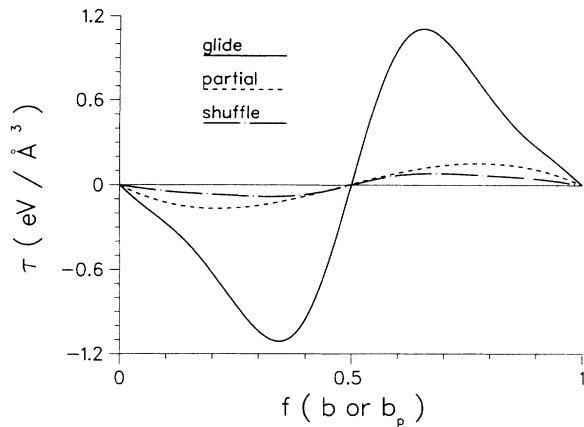


FIG. 4. Restoring forces  $\tau$  corresponding to the  $\gamma$  surface sections of Fig. 3.

Silicon is an anisotropic crystal, so procedures outlined by Hirth and Lothe<sup>17</sup> for such a situation had to be followed. For the Burgers vectors of interest, which all lie in the  $\{111\}$  plane, the  $K$  values obtained can be expressed in terms of effective elastic constants  $\mu$  and  $\nu$  for the  $\{111\}$  plane. In other words, within the  $\{111\}$  plane silicon is essentially isotropic. The values derived within the  $\{111\}$  plane are  $\mu' = 6.375 \times 10^{11}$  dyn/cm<sup>2</sup> and  $\nu' = 0.2561$ . This is to be compared with quoted averaged values for Si,  $\mu = 6.81 \times 10^{11}$  dyn/cm<sup>2</sup> and  $\nu = 0.218$ .<sup>17</sup>

As mentioned in the preceding section the restoring forces were obtained from the  $\gamma$  surface, the energy variation of the gsf with displacement. To integrate these forces into the calculation they were fitted with a sine series for the  $\langle 110 \rangle$  dislocations and exponentials for the  $\langle 112 \rangle$  dislocations. In this latter direction the interval of force field of interest is not periodic. One goes from an equilibrium position to a stable stacking-fault position. The disregistry  $f(x)$  was obtained by searching for a solution in the form

$$f(x) = \frac{b}{\pi} \sum_{i=1}^N \alpha_i \arctan \frac{x - x_i}{c_i} + \frac{b}{2}, \quad (13)$$

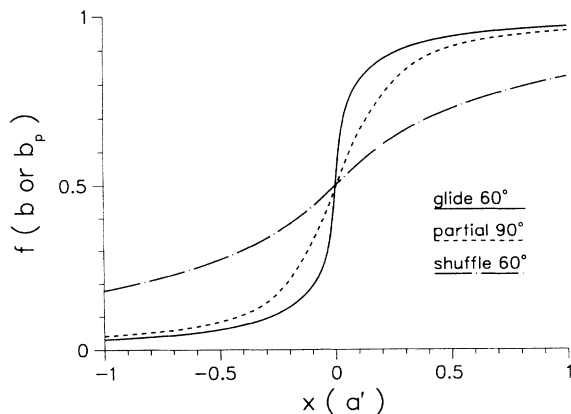


FIG. 5. Typical dislocation profiles. Displacements along the Burgers vectors plotted as a function of the distance from the dislocation line.

where  $\alpha_i$ ,  $x_i$ , and  $c_i$  are variational constants and  $N$  is an integer.<sup>28,29</sup> The normalization condition given in Eq. (6) leads to the sum rule

$$\sum_{i=1}^N \alpha_i = 1, \quad (14)$$

where every  $\alpha_i$  is a positive number. Substituting the above trial function into the left-hand side of the PN equation gives

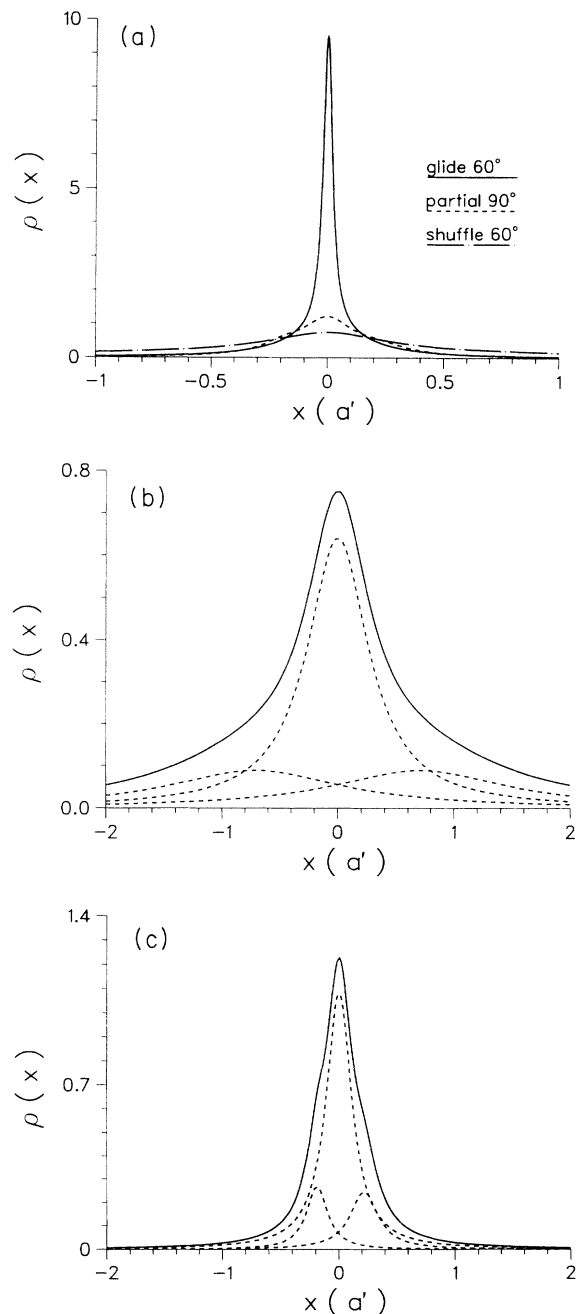


FIG. 6. Some dislocation densities  $\rho(x) = df(x)/dx$ ; (a) compares the distribution for three dislocations; (b) and (c) show the contributions from the three terms in Eq. (13) (dashed lines) for the 60° shuffle and 90° partials, respectively (full lines are the sum of the dashed lines).

$$F'_b(x) = Kb \sum_{i=1}^N \alpha_i \frac{x - x_i}{(x - x_i)^2 + c_i^2}. \quad (15)$$

The constants  $\alpha_i$ ,  $c_i$ , and  $x_i$  are obtained by minimizing the expression

$$\Delta = |F'_b(\alpha_i, c_i, x_i; x) - F_b(f(\alpha_i, c_i, x_i))|. \quad (16)$$

$N=3$  was found to be sufficient to provide a good fit.

Table I shows the input data for the four dislocations considered and their calculated widths. Some typical dislocation profiles are shown in Fig. 5. Corresponding dislocation densities appear in Fig. 6. This last figure also shows the contribution of each term in Eq. (13) for two of the dislocations.

Not surprisingly, since the width  $\xi$  is essentially inversely proportional to the maximum of the restoring stress  $\tau_{\max}$  the shuffle dislocation widths are an order of magnitude larger than the glide dislocation widths. The shuffle dislocation profile is nearly that of a PN dislocation with sinusoidal restoring stress. The glide partials have slightly larger widths than the full glide dislocations. The departures from sinusoidal behavior in the restoring stresses are reflected in the dislocation densities most visibly in the one for the  $90^\circ$  partial in Fig. 6(c).

#### V. MISFIT ENERGIES, PEIERLS-NABARRO ENERGIES, AND STRESSES

Although a periodic restoring force has been incorporated into the PN model, it still considers the crystal above and below the glide plane as an elastic continuum medium. As in the Frank and van der Merwe model<sup>24</sup> the dislocation is free to glide in the crystal. If  $f(x)$  is a solution to the displacement field, so is  $f(x-u)$ , where  $u$  is any constant [ $f(x-u)$  corresponds to a dislocation translated by  $u$ ]. This "continuum-mass" dislocation has no PN stress. However, a stress can be defined by noting that the displacement function  $f(x-u)$  corresponds to a real displacement only where an atomic plane is present. In the absence of a dislocation the spacing of atomic planes in the direction  $x$  is  $a'$ . With the  $x$  axis along a  $\langle 112 \rangle$  direction  $a' = (\sqrt{6}/4)a = 3.33 \text{ \AA}$ , where  $a$  is the Si lattice constant  $5.43 \text{ \AA}$ . When the dislocation is introduced, the planes, in the upper half of the crystal at a position  $ma'$  in a direction perpendicular to the dislocation line, will be displaced with respect to the lower half by  $f(ma'-u)$ . The misfit energy can be considered as the sum of misfit energies between pairs of atomic planes and can be written

$$W(u) = \sum_{m=-\infty}^{+\infty} \gamma(f(ma'-u))a'. \quad (17)$$

This formula focuses on the variation of the disregistry as one moves across the dislocation core along the interface in a direction perpendicular to the dislocation line. It has the correct period  $a'$  (see Fig. 7), and the right limit for very narrow dislocations for which the amplitude of variation of  $W(u)$ ,  $W_p$  should be the same as that of  $\gamma(u)a'$ , i.e.,  $\gamma_{\max}a'$ .<sup>30</sup>  $W_p$ , the PN energy, is the energy barrier for motion of the dislocation. A physically related quan-

tity is the Peierls stress  $\sigma_p$ , the maximum stress required to overcome the barrier. Two energy barriers may be comparable, but if the distances are quite different over which this energy rise has to be realized, the corresponding Peierls stresses can be quite different. A longer repeat distance will usually necessitate a smaller Peierls stress. Our formula has the correct period for  $W(u)$  and hence is expected to give a reasonable value for  $\sigma_p$ .  $\sigma_p$  is defined as the maximum in the variation of the interface stress,  $\sigma$ , the scaled slope of  $W(u)$  for a given position of the dislocation:

$$\sigma_p = \max\{\sigma\} = \max\left\{\frac{1}{a'} \frac{dW}{du}\right\}. \quad (18)$$

It is obtained directly from Fig. 8.

An estimate for very narrow dislocations, where the core is less than one lattice site wide can be easily derived using the continuum dislocation profile given in Eq. (11) with an adjustable width  $\xi$ . Since only one term in the sum in Eq. (17) will contribute significantly:

$$\begin{aligned} \sigma_p &= \max\left\{\frac{d\gamma(f(-u))}{du}\right\} \\ &= \max\left\{-\frac{d\gamma}{df} \frac{df}{du}\right\} \approx \tau_{\max} \frac{b}{\pi\xi} \approx 4 \frac{\tau_{\max}^2}{K}. \end{aligned} \quad (19)$$

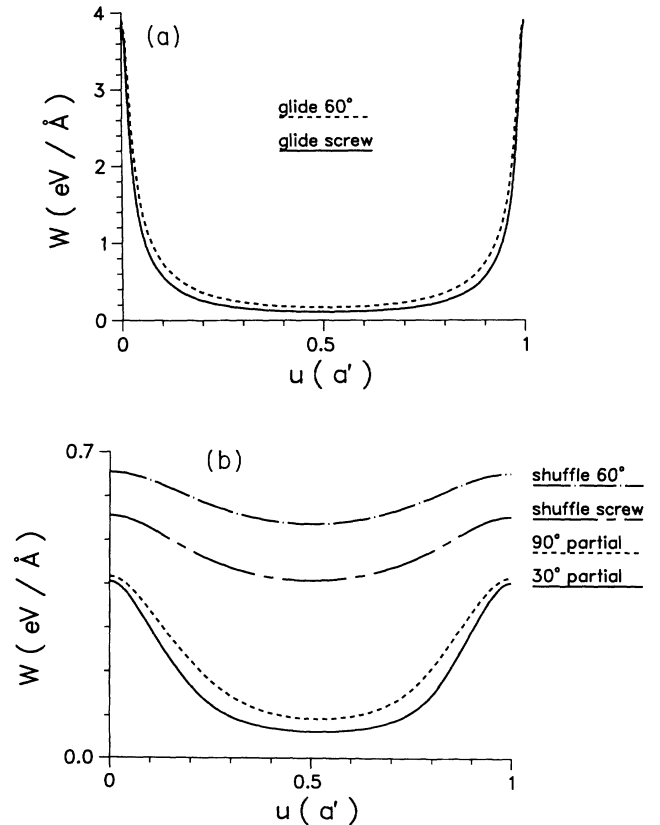


FIG. 7. Misfit energies  $W(u)$  for (a) full dislocations in the glide plane and (b) full dislocations in the shuffle plane and partials in the glide plane.

TABLE II. Properties of dislocations in Si obtained from the Peierls-Nabarro model ( $\mu=0.4$  eV/Å<sup>3</sup>).

Dislocation		$W_m$ (eV/Å)	$W(a'/2)$ (eV/Å)	$W_p$ (eV/Å)	$\sigma_p$ ( $\mu$ )
Glide	60°	0.588	0.169	3.77	18.02
	Screw	0.468	0.110	3.74	22.67
Shuffle	60°	0.588	0.538	0.116	0.088
	Screw	0.468	0.408	0.148	0.119
Glide	30°	0.169	0.062	0.343	0.374
Partials	90°	0.210	0.093	0.323	0.300

Whereas the PN energy depends in this limit only on the potential barrier to be overcome in the  $\gamma$  surface, the Peierls stress is very sensitive to the width of the dislocation or the relative strength of the lattice with respect to the energy barrier.

Typical variations of  $W(u)$  are shown in Fig. 7. The minimum  $W(a'/2)$  can be viewed as a misfit energy. It is the total energy stored across the glide surface. It is the nonelastic part of the dislocation energy and provides an estimate for the core energy of the dislocation, which takes into account the discreteness of the lattice. It is different from the obvious definition of this quantity in the PN model, which is the integral of the disregistry energy over the whole interface:

$$W_m = \int_{-\infty}^{+\infty} \gamma(f(x)) dx. \quad (20)$$

This last quantity can be shown to be independent of the restoring force. Integration by parts and use of the PN equation gives

$$\begin{aligned} W_m &= - \int_{-\infty}^{+\infty} x \frac{\partial \gamma}{\partial x} dx \\ &= - \int_{-\infty}^{+\infty} x \frac{\partial \gamma(f(x))}{\partial f} \frac{\partial f}{\partial x} dx \\ &= \frac{K}{2\pi} \int \int \frac{x}{x'-x} \frac{\partial f}{\partial x'} \frac{\partial f}{\partial x} dx dx'. \end{aligned} \quad (21)$$

$$= \frac{K}{2\pi} \int \int \frac{x}{x'-x} \frac{\partial f}{\partial x'} \frac{\partial f}{\partial x} dx dx'. \quad (22)$$

Separating this last integral into two equal parts with an interchange in the roles of  $x$  and  $x'$  yields:

$$W_m = \frac{K}{4\pi} \int \int \frac{\partial f}{\partial x} \frac{\partial f}{\partial x'} dx dx' = \frac{Kb^2}{4\pi}. \quad (23)$$

$W_m$  depends only on the elastic properties of the material and the Burgers vector. The integral reflects the fact earlier noted that the material on each side of the glide plane is taken as a continuum. The restoring forces determine the spreading of this energy over a larger or smaller area but, since the medium is elastic, the total remains unchanged.  $W_m$ , therefore, does not distinguish between glide or shuffle plane dislocations. It is interesting to note that  $W_m$  is the average of the function  $W(u)$ , since

$$\begin{aligned} \frac{1}{a'} \int_0^{a'} W(u) du &= \int_0^{a'} \sum_{m=-\infty}^{+\infty} \gamma(fma' - u) du \\ &= \int_{-\infty}^{+\infty} \gamma(f(u)) du = W_m. \end{aligned} \quad (24)$$

$W_m$  is, hence, an average misfit energy for all positions of

the dislocations as it is displaced through the lattice. As mentioned earlier  $W(a'/2)$ , an estimate of the core energy, is the minimum and  $W_p$ , the PN energy, the amplitude of the variation of  $W(u)$ .

The results for all these quantities are shown in Table II for the Si dislocations. As this table shows for a particular dislocation, glide and shuffle sets have the same average misfit energy because that energy depends only on the elastic response of the lattice. For the narrow glide set, this energy has a larger amplitude than for the wide shuffle set. Consequently glide dislocations have

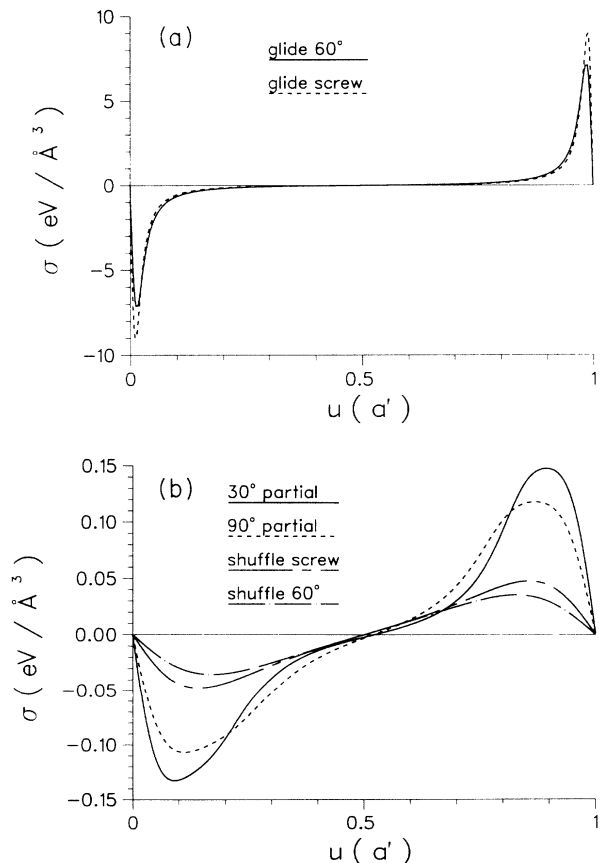


FIG. 8. Interface stresses  $\sigma$  corresponding to the variation of the misfit  $W(u)$  energy with position  $u$ . The maximum corresponds to the Peierls stress  $\sigma_p$ . As in Fig. 7, (a) for full dislocations in the glide plane and (b) for full dislocations in the shuffle plane and partial dislocations in the glide plane.

larger PN energies and Peierls stresses than the shuffle dislocations. Another consequence is that, since more atomic planes are deformed in the shuffle dislocations, its total minimum misfit or core energy is larger than that of the glide dislocations, where only a couple of planes are affected. These results follow from the relationship developed above between  $W_p$  and the core energy  $W(a'/2)$ . It will be interesting to see if atomistic computer simulations will verify that.

## VI. DISCUSSION AND CONCLUSION

Our calculations suggest that, in Si at 0 K, shuffle-set dislocations should be easier to form and move than those belonging to the glide set. However, experimental observations show that total dislocations in Si are dissociated into partial dislocations separated by an intrinsic stacking fault. Since this fault can exist only on glide planes, the general wisdom is that mobile dislocations belong to the glide set (although it has been argued that this inference is not without question<sup>6</sup>). These statements are not necessarily incompatible. It has been shown that, in principle, a shuffle dislocation can decompose into a dissociated glide set dislocation plus a row of point defects.<sup>3</sup> The representation of such a complex lies beyond the PN model, but it is likely that motion, which will occur either on the glide plane by dragging or dropping the point defect row, or on the shuffle plane by recombination prior to glide, will be no easier than the motion of a glide set dislocation. It is also possible that finite temperature effects may alter the conclusions of the calculations. Kaxiras and Duesbery<sup>11</sup> have shown that if the entropy is taken account, then above a critical temperature and in the presence of a tensile stress, the free energy of the unstable stacking fault  $\gamma_{us}$  can become lower on the glide planes than on the shuffle set. The resolution of this problem will be the subject of future work.

The calculated PN stresses can be related to the experi-

mental data available on dislocation mobility. The motion of simple individual dislocations cannot be studied. What are followed are dislocation loops formed of segments of various types of structures either perfect or dissociated dislocations. There is a belief that both shuffle and glide types are involved in the loops. As discussed in Sec. II, there is conclusive evidence that the 90° partials are more mobile than 30° partials, and this agrees with our findings even when the stacking-fault creation force  $0.01\mu$  is taken into account. This stacking fault creation force is small.

The PN model has limitations. Most noticeably, when the dislocations are very narrow, treating the response of the lattice above and below the glide plane as elastic may underestimate the forces and energies near the core. In spite of this the PN model gives us an appreciation of the interplay of the forces determining the properties of the various dislocations. In particular, it gives simple relationships between the width of a dislocation, the corresponding relevant elastic constants of the solid and the strength of the restoring force as provided by the generalized stacking fault (gsf) surface. In as much as the key physical assumptions of the model referring to the form of the core as planar are correct, this model is expected to give the correct relationship between gsf surface characteristics and the properties of dislocations at low temperature.

## ACKNOWLEDGMENTS

We would like to thank E. Kaxiras for providing us with his values for the generalized stacking-fault potential and for useful comments on the manuscript. This work has been supported by the Natural Sciences and Engineering Research Council of Canada (B.J.), the Office of Naval Research under Contract No. N00014-91-C-0067 (M.S.D.) and the Ontario Government through financial assistance for Q.R.

\*Electronic address: BJOSJ@ACADVM1.UOTTAWA.CA

†Electronic address: REN@PHYSICS.UOTTAWA.CA

‡Electronic address: DUESBERY@NRL.NAVY.MIL

<sup>1</sup>D. C. Houghton, J.-P. Noël, N. L. Rowell, and D. D. Perovic, in *Multicomponent and Multilayered Thin Films for Advanced Microtechnologies: Techniques, Fundamentals, and Devices*, Vol. 234 of *NATO Advanced Study Institute, Series E: Applied Sciences*, edited by O. Auciello and J. Engemann (Kluwer, Dordrecht, 1993), p. 401.

<sup>2</sup>H. Alexander, in *Solid State Physics*, edited by F. Seitz, D. Turnbull, and H. Ehrenreich (Academic, New York, 1968), Vol. 22, p. 27.

<sup>3</sup>S. Amelinckx, in *Dislocations in Solids*, edited by F. R. N. Nabarro (North-Holland, Amsterdam, 1979), Vol. 2, p. 294.

<sup>4</sup>H. Alexander, in *Dislocations in Solids*, edited by F. R. N. Nabarro (North-Holland, Amsterdam, 1986), Vol. 7, p. 114.

<sup>5</sup>A. George and J. Rabier, *Rev. Phys. Appl.* **22**, 941 (1987).

<sup>6</sup>F. Louchet and J. Thibault-Desseaux, *Rev. Phys. Appl.* **22**, 207 (1987).

<sup>7</sup>M. S. Duesbery and G. Y. Richardson, *CRC Crit. Rev. Solid State Mater. Sci.* **17**, 1 (1991).

<sup>8</sup>M. S. Duesbery, D. J. Michel, and B. Joós, *Mater. Res. Soc. Symp. Proc.* **163**, 941 (1990).

<sup>9</sup>M. S. Duesbery, B. Joós, and D. J. Michel, *Phys. Rev. B* **43**, 5143 (1991).

<sup>10</sup>M. S. Duesbery, D. J. Michel, E. Kaxiras, and B. Joós, *Mater. Res. Soc. Symp. Proc.* **209**, 125 (1991).

<sup>11</sup>E. Kaxiras and M. S. Duesbery, *Phys. Rev. Lett.* **70**, 3752 (1993).

<sup>12</sup>V. Vitek, L. Lejček, and D. K. Bowen, in *Proceedings of the Batelle Colloquium on Interatomic Potentials and Simulation of Lattice Defects, Seattle, 1971*, edited by P. C. Gehlen, J. R. Beeler Jr., and R. I. Jaffee (Plenum, New York, 1972), p. 493.

<sup>13</sup>V. Vitek and M. Yamaguchi, *J. Phys. F* **3**, 537 (1973).

<sup>14</sup>M. Yamaguchi and V. Vitek, *J. Phys. F* **5**, 11 (1975).

<sup>15</sup>R. Peierls, *Proc. Phys. Soc. London* **52**, 34 (1940).

<sup>16</sup>F. R. N. Nabarro, *Proc. Phys. Soc. London* **59**, 256 (1947).

<sup>17</sup>J. P. Hirth and J. Lothe, *Theory of Dislocations*, 2nd ed. (Wiley, New York, 1982).

<sup>18</sup>I. L. F. Ray and D. J. H. Cockayne, *Proc. R. Soc. London, Ser. A* **325**, 543 (1971).

<sup>19</sup>K. Wessel and H. Alexander, *Philos. Mag.* **35**, 1523 (1977).

- <sup>20</sup>H. Alexander, H. Gottschalk, and C. Kisielowski-Kemmerich, in *Dislocations in Solids*, edited by H. Suzuki, T. Ninomoya, K. Sumino, and S. Takeuchi (University of Tokyo Press, Tokyo, 1985), p. 337.
- <sup>21</sup>P. Grosbras, J. L. Demenet, H. Garem, and J. C. Desoyer, *Phys. Status Solidi A* **84**, 481 (1984).
- <sup>22</sup>J. L. Demenet, P. Grosbras, H. Garem, and J. C. Desoyer, *Philos. Mag. A* **59**, 501 (1989).
- <sup>23</sup>J. Frenkel and T. Kontorowa, *Phys. Z. Sowjetunion* **13**, 1 (1938).
- <sup>24</sup>F. C. Frank and J. H. van der Merwe, *Proc. R. Soc. London, Ser. A* **198**, 205 (1949).
- <sup>25</sup>R. Hobart, *J. Appl. Phys.* **36**, 1944 (1965); B. Joós, *Solid State Commun.* **42**, 709 (1982).
- <sup>26</sup>A. Foreman, M. A. Jaswon, and J. K. Wood, *Proc. Phys. Soc. A* **64**, 156 (1951).
- <sup>27</sup>J. W. Christian and V. Vitek, *Rep. Prog. Phys.* **33**, 307 (1970).
- <sup>28</sup>L. Lejček, *Czech. J. Phys. B* **22**, 802 (1972).
- <sup>29</sup>F. Kroupa and L. Lejček, *Czech. J. Phys. B* **22**, 813 (1972).
- <sup>30</sup>Our formula is the same as the one suggested by Christian and Vitek (Ref. 27) but is different from the one discussed in Ref. 17 and originally due to Peierls (Ref. 15) and Nabarro (Ref. 16). That formula is based on a slightly different atomistic basis of the continuum model leading to sums for the upper and lower half planes with coordinates differing by  $a'/2$ . The disadvantage of that formula is that both  $u=0$  and  $a'/2$  correspond to maximum energy configurations and the minimum energy configuration is an asymmetric configuration with  $u=a'/4$ , resulting in a period for  $W(u)$  of  $a'/2$  instead of  $a'$ .